Unconventional superconductivity and quantum criticality in the heavy fermions $CeIrSi_3$ and $CeRhSi_3$

J. F. Landaeta,[1,2] D. Subero,[1] D. Catalá,[1,2] S. V. Taylor,[1,3] N. Kimura,[4] R. Settai,[5] Y. Ōnuki,[6] M. Sigrist,[7] and I. Bonalde[1]

[1]*Centro de Física, Instituto Venezolano de Investigaciones Científicas, Apartado 20632, Caracas 1020-A, Venezuela*

[2]*Departamento de Física, Facultad de Ciencias, Universidad Central de Venezuela, Apartado 47586, Caracas 1041-A, Venezuela*

[3]*Cavendish Laboratory, Cambridge University, JJ Thomson Avenue, Cambridge CB3 OHE, United Kingdom*

[4]*Department of Physics, Graduate School of Science, Tohoku University, Sendai 980-8578, Japan*

[5]*Department of Physics, Niigata University, Niigata 950-2181, Japan*

[6]*Faculty of Science, University of the Ryukyus, Nishihara, Okinawa 903-0213, Japan*

[7]*Institute for Theoretical Physics, ETH Zürich, CH-8093, Zürich, Switzerland*

(Received 28 September 2017; revised manuscript received 9 March 2018; published 28 March 2018)

In most strongly correlated electron systems superconductivity appears nearby a magnetic quantum critical point (QCP) which is believed to cause unconventional behaviors. In order to explore this physics, we present here a study of the heavy-fermion superconductors $CeIrSi_3$ and $CeRhSi_3$ carried out using a newly developed system for high-resolution magnetic penetration-depth measurements under pressure. Superconductivity in $CeIrSi_3$ shows a change from an excitation spectrum with a line-nodal gap to one which is entirely gapful when pressure is close but not yet at the QCP. In contrast, $CeRhSi_3$ does not possess a $T = 0$ quantum phase transition and the superconducting phase remains for all accessible pressures with a nodal gap. Combining both results suggests that in these compounds unconventional superconducting behaviors are rather connected with the coexisting antiferromagnetic order. This study provides another viewpoint on the interplay of superconductivity, magnetism, and quantum criticality in $CeIrSi_3$ and $CeRhSi_3$ and maybe in other heavy fermions.

DOI: 10.1103/PhysRevB.97.104513

I. INTRODUCTION

Magnetic order is a common phenomenon in a wide range of strongly correlated electron systems (SCES) such as high-T_c cuprates [1], organics [2], iron pnictides/chalcogenides [3], and heavy fermions [4,5]. Intriguingly the weakening of magnetic order by a tuning parameter—as pressure, chemical substitution, or magnetic field—promotes the emergence of a superconducting phase which is thought to be unconventional and be influenced by the magnetic QCP (where the transition temperature of the magnetic order vanishes). In few cases such as the hole-doped cuprates, the antiferromagnetic (AFM) phase disappears before superconductivity rises [1]. The most usual situation, however, is a "superconducting dome" around the QCP where the critical temperature T_c takes a maximum value. This implies that antiferromagnetism coexists with superconductivity in part of the dome region. Although QCP has been thought to be related to superconductivity, it has not been experimentally linked to unconventional behaviors. We note that unconventional superconductivity is defined as the breaking of additional symmetries besides the gauge U(1). A quite common but not mandatory result of unconventional superconductivity is the presence of nodes in the energy gap. Sometimes nodes or other unconventional-type behaviors are accidental (not imposed by symmetry), in which case superconductivity can still be conventional. The connection between unconventionality and QCP remains a relevant and long-standing issue.

Studies of the superconducting energy gap structure—as a fingerprint for conventional or unconventional pairing—are usually carried out using, besides direct spectroscopic methods, thermodynamic/electromagnetic probes. It is not always possible employing these techniques to determine whether a nodal structure is symmetry protected or accidental. Analyses of the gap have been performed across the dome in very few SCES [6–10]. The present research aims to gain more insight into the behavior of superconductivity near a magnetic QCP by examining the excitation spectrum of noncentrosymmetric heavy fermions $CeIrSi_3$ and $CeRhSi_3$.

$CeIrSi_3$ goes to an antiferromagnetic spin-density-wave (SDW) state below the Néel temperature $T_N = 5.0$ K at ambient pressure [11]. As pressure increases T_N decreases monotonically toward zero and an AFM-SDW QCP is expected around 2.5 GPa. Superconductivity sets in about 1.3 GPa and persists up to 3.5 GPa with a maximum critical temperature of 1.6 K at $p_c^* \approx 2.58$ GPa [12]. So far, the AFM order has not been detected inside the superconducting phase above the critical pressure $p_c = 2.25$ GPa at which $T_N = T_c$. A slightly different situation is encountered in $CeRhSi_3$, which becomes an SDW antiferromagnet below $T_N = 1.6$ K at ambient pressure [13]. Upon increasing pressure T_N passes through a maximum at 1.9 K and then decreases smoothly and approaches asymptotically the superconducting dome at its top at $p_c^* \approx 2.8$ GPa. In $CeRhSi_3$ T_N does not head toward zero, meaning that it may lack a magnetic QCP. Very few experimental analysis of the pairing symmetry have been performed in these compounds. In an NMR relaxation-rate study at 2.6 GPa no coherence peak and a $1/T_1 \sim T^3$ response below T_c was observed, consistent with line nodes in the gap structure [14]. A possible presence of nodes was also suggested

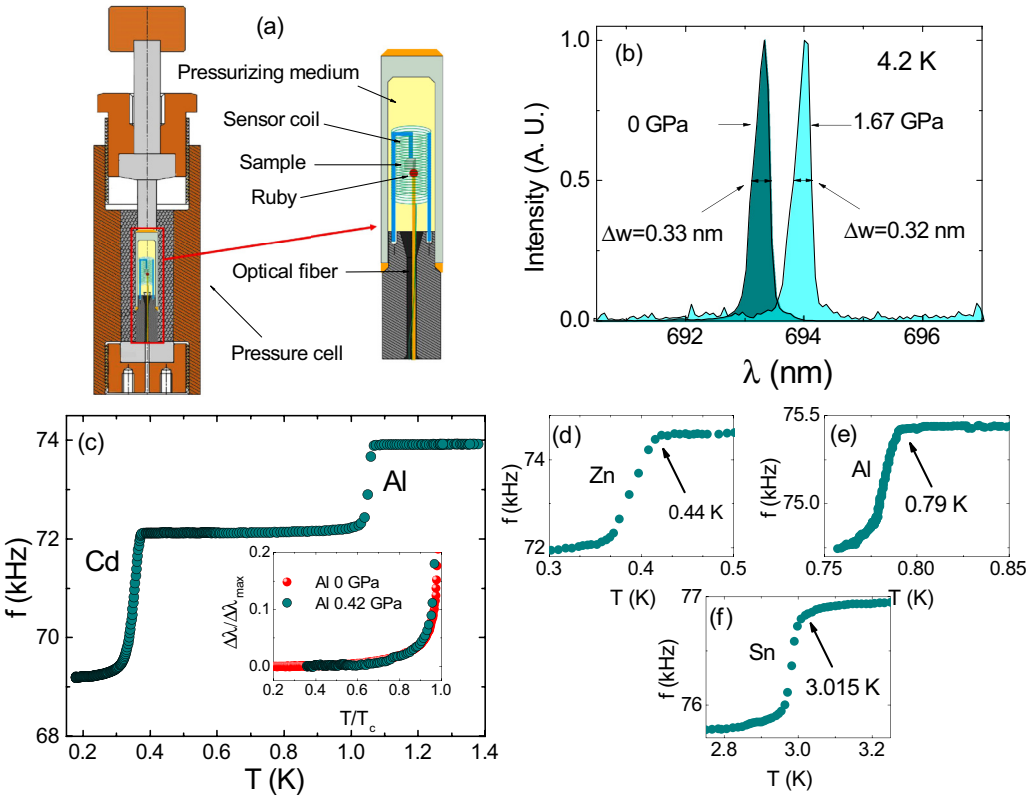

FIG. 1. (a) Schematic of the pressure cell plus the sensing system for penetration-depth measurements at high pressures and low temperatures. (b) Ruby fluorescence spectra for 0 and 1.67 GPa at 4 K indicating good hydrostaticity of glycerol. (c) Signals of Cd and Al at 0.42 GPa showing correct values of T_c and a good response of the system. Inset compares the Al data (blue) with those taken in an ambient-pressure system (red) [17]. (d)–(f) Signals of Zn, Al, and Sn at 1.67 GPa displaying expected critical temperatures.

in a brief analysis at 2.6 GPa on field-angle resolved specific heat measurements [15]. Another hint at the type (conventional/unconventional) of superconductivity comes from tests of the parity and spin state of the pairing via measurements of the upper critical field H_{c2}. The extremely high values of H_{c2} (∼30–40 T) found in $CeIrSi_3$ and $CeRhSi_3$ at pressures around 2.6 GPa may point at first to unconventional pairing states [16]. However, in these noncentrosymmetric compounds the spin-orbit coupling may complicate the interpretation of all these results [16]. Up to now the pairing state remains undisclosed in both materials.

Here we study $CeIrSi_3$ and $CeRhSi_3$ under hydrostatic pressure up to 2.81 GPa and temperatures down to 200 mK by means of the magnetic penetration depth $\lambda(T)$, which is widely considered one of the most sensitive probes to determine the energy gap structure or symmetry the order parameter. Our results reveal a crossover from nodal to isotropic gap in $CeIrSi_3$ and a nodal gap in $CeRhSi_3$ along the pressure range studied.

II. EXPERIMENTAL METHODS

A. Sample preparation

Single crystals were grown by the Czochralski method in tetra-arc furnaces [11,13]. Grown ingots of $CeIrSi_3$ were wrapped in Ta foil, sealed in a quartz tube under a vacuum of 10^{-6} Torr, and annealed at 950 °C for 5 days. For $CeRhSi_3$ the starting materials were 4N-Ce, 3N-Rh, and 5N-Si and the resulting ingots were annealed at 900 °C under a vacuum of 2×10^{-6} Torr for a week. Typical residual resistivity ratios were 120 for $CeIrSi_3$ and 180 for $CeRhSi_3$.

B. Experimental setup

Measurements were performed using a 13 MHz tunnel diode oscillator [17] coupled to a self-clamped hybrid-piston-cylinder cell made of nonmagnetic CuBe, WC, and NiCrAl alloys (C&T Factory Co., Ltd.), as schematically shown in the left panel of Fig. 1(a). A 2.0-mm-diameter Cu-wire coil with a 7.2-mm winding height was placed into the 4.0-mm-diameter inner space of the cell filled with a pressure-transmitting medium, as sketched in the right panel of Fig. 1(a). Samples were attached, with a fast-bonding glue, to a tiny plastic rod fitted inside the coil. The coil and the plastic rod were thermally anchored to the pressure cell, which was mounted to the mixing chamber of a dilution refrigerator. Samples were aligned with the *ab* plane perpendicular to the probing magnetic field of less than 5 mOe, so we sensed the in-plane penetration depth. A thermometer was located close to the attaching point of the plastic rod at the pressure cell.

A fiber-optic setup that allows one to measure the ruby R1 fluorescence line shifts was employed for estimating pressure at 4 K. Ruby crystals were fixed—also with a fast-bonding glue—to the end of an optical fiber and placed near the sample inside the coil, as shown in the right panel of Fig. 1(a). We found that glycerol was the most appropriate pressure-transmitting

medium because of its better thermal conductivity at temperatures below 1 K. It was previously demonstrated that glycerol loses its hydrostaticity only above 5 GPa [18], a value which is significantly above our working range. In any case, in Fig. 1(b) we exhibit the ruby R1 fluorescence spectra at 4 K for 0 and 1.67 GPa. No difference is observed in the linewidths, one of the parameters commonly used as a hydrostaticity probe [18]. We determined pressure with the expression [19] $P(\mathrm{GPa}) = A_0 \ln(\frac{\lambda}{\lambda_0})$, where $A_0 = 1762$ GPa and the wavelength $\lambda_0 = 693.33$ nm. Our spectrograph has a resolution of 0.015 nm, which leads to a pressure error of 0.04 GPa.

The experimental system was tested by measuring high-purity tin, aluminum, zinc, and cadmium samples. All runs at different pressures yielded the expected results. Figure 1(c) displays $\lambda(T)$ for Cd and Al mounted together at 0.46 GPa. The inset compares the Al data with those taken in an ambient-pressure system. No significant difference is observed. Figures 1(d)–1(f) exhibit $\lambda(T)$ for Zn, Al, and Sn at 1.67 GPa. All critical temperatures coincide with the ones obtained earlier [20,21], indicating a correct measurement of both temperature and pressure. No appreciable background signal was detected in the range scanned.

C. Magnetic penetration depth and skin depth

In the normal state above T_c, which we define as the onset of the diamagnetic response, our experimental setup probes the skin depth; i.e., $f(T) \propto \delta(T) = \sqrt{2\rho(T)/\mu(T)\omega}$. Here $\rho(T)$ is the resistivity, $\mu(T)$ is the permeability, and $\omega = 2\pi f$ is related to the oscillator frequency f. In the case of the magnetic superconductors $CeIrSi_3$ and $CeRhSi_3$, below T_c the effective penetration depth is given by $\lambda(T) = \sqrt{\mu(T)}\lambda_L(T)$, where $\lambda_L(T) = \sqrt{n_0/n_s(T)}c/\omega_p$. Here ω_p is the plasma frequency, c is the speed of light, n_0 is the carrier density, and n_s is the superconducting electron density. In the low-temperature limit $\mu(T)$ of antiferromagnets approaches 1 exponentially [22,23], such that we directly probe the Cooper-pair density as $f(T) \propto \lambda(T) = \lambda_L(T)$. The variation of the measured frequency from its value at the lowest temperature, $\Delta f(T)$, is directly proportional to the penetration-depth shift $\Delta\lambda(T)$ below T_c.

III. RESULTS AND DISCUSSION

Figures 2(a)–2(h) show $f(T)$ for $CeIrSi_3$ at different pressures. Apart from the superconducting transitions indicated by T_c, the skin depth displays a marked change of slope at points labeled with T_N in Figs. 2(a)–2(c). We attribute these anomalies to AFM transitions, as the change occurs in each case near the reported T_N [11]. We remark that these anomalies in the skin depth can reflect the temperature response of resistivity and permeability.

Our measurements in $CeIrSi_3$ also show signs of the AFM phase when $T_N < T_c$. We argue that the bump at the transition at 2.31 GPa [Fig. 2(d)] and the upturns observed at very low temperatures at 2.38 and 2.52 GPa [Figs. 2(e) and 2(f)] are likely signatures of the low-temperature AFM order or fluctuations near p_c^*. The emergence of antiferromagnetism inside superconductivity causes Cooper-pair breaking that appears in penetration depth as a paramagnetic signal [24–27]. Since the upturns are only seen at some pressures, magnetic

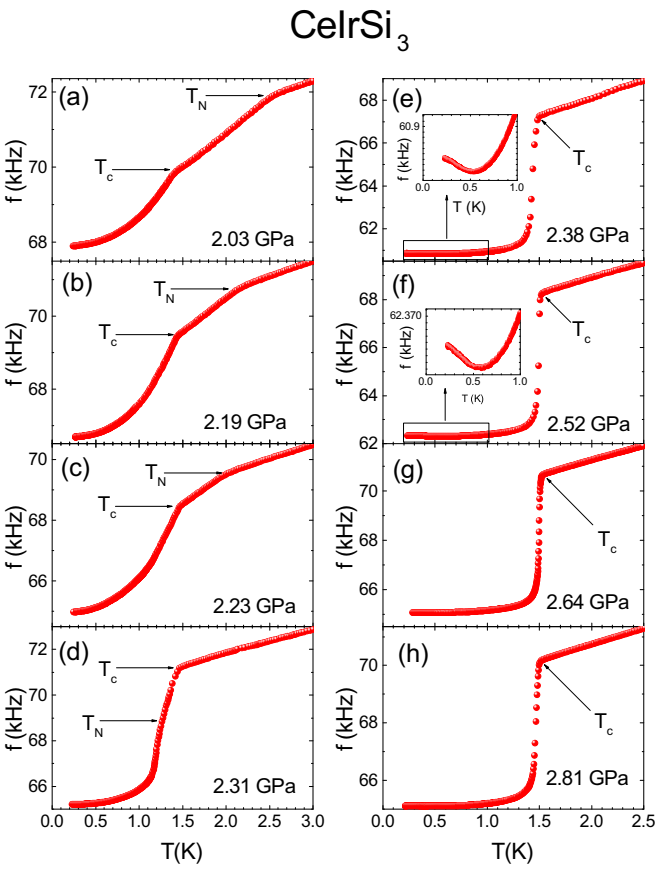

FIG. 2. Oscillator frequency, proportional to the penetration depth at $T < T_c$ and the skin depth at $T > T_c$, for $CeIrSi_3$ at different pressures. T_c marks the onset of the superconducting transitions and T_N is associated with AFM transitions, in accordance with previous measurements. Insets of (e) and (f) show upturns around 0.4 K related to pair-breaking paramagnetic precursors of an AFM transition.

impurities and Andreev bound states are ruled out as the cause of their occurrences. Moreover, the fact that the upturns appear once the superconducting contribution is clearly exponential (indicative of an isotropic energy gap) further discards Andreev states. This detection of the AFM phase when $T_N < T_c$ is in line with earlier evidence in another heavy fermion [28].

Figures 3(a)–3(i) display $f(T)$ for $CeRhSi_3$ at different pressures. The skin depth exhibits slope changes at points denoted by T_N in Figs. 3(a)–3(g), which agree with previously reported AFM transitions in $CeRhSi_3$ [13]. Contrary to the observation in $CeIrSi_3$, no trace of an AFM phase is detected below T_c in $CeRhSi_3$.

A. Phase diagrams of $CeIrSi_3$ and $CeRhSi_3$

We used our own T_c's and T_N's and other reported values [11,12,29,30] to construct the T-P phase diagrams of $CeIrSi_3$ and $CeRhSi_3$ displayed in Figs. 4(a) and 4(b), respectively. The general agreement of the $CeIrSi_3$ data is remarkable, whereas no concurrence in the T_c values is found in $CeRhSi_3$. The large data scattering at $p < 2.0$ GPa in $CeIrSi_3$ is due to difficulties in defining the critical temperatures from the very broad transitions occurring at those pressures. On the other hand, we think that the inconsistency of T_c in $CeRhSi_3$ may be

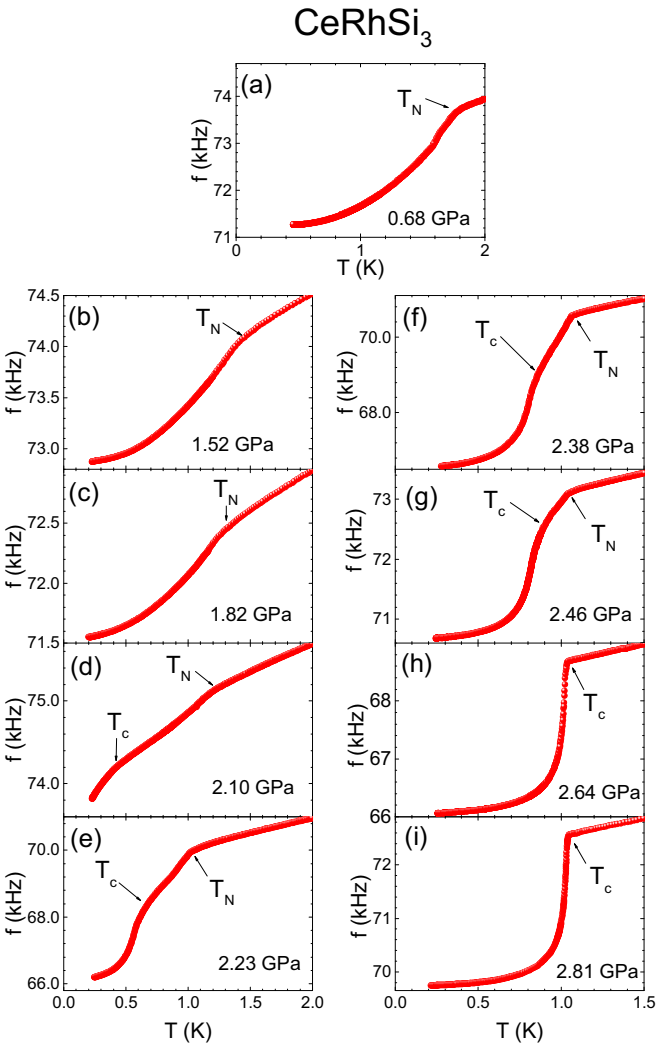

FIG. 3. Oscillator frequency for $CeRhSi_3$ at different pressures. T_c and T_N mark the onsets of superconducting and AFM transitions, respectively.

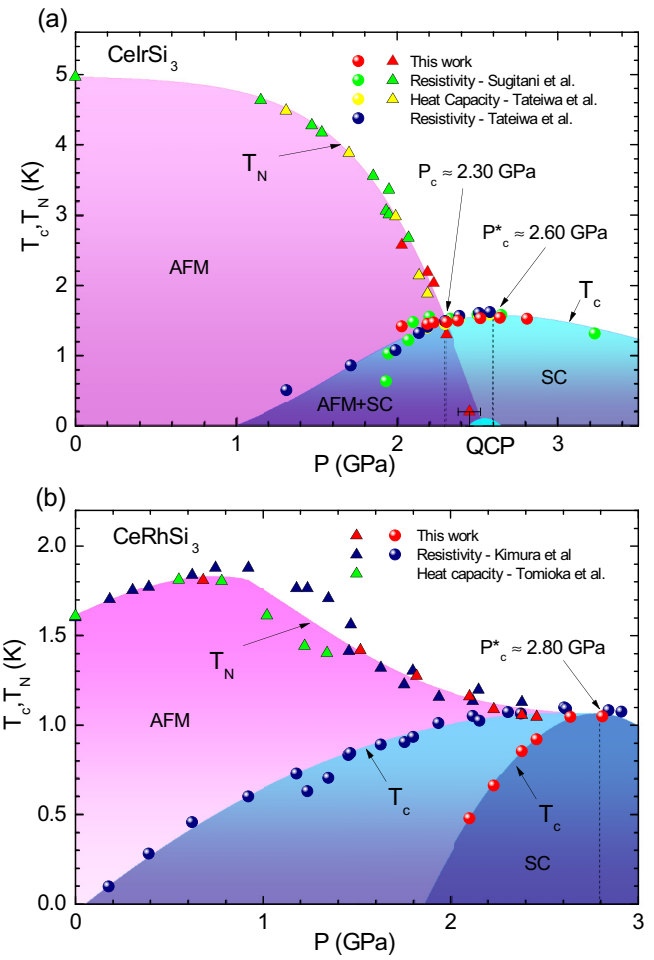

FIG. 4. T-P phase diagrams of (a) $CeIrSi_3$ and (b) $CeRhSi_3$ composed of our data and others previously reported. Triangles and spheres represent Néel and superconducting critical temperatures, respectively. In $CeIrSi_3$ a QCP occurs at p_c^*. No $T = 0$ quantum phase transition is seen in $CeRhSi_3$. Our T_c data in $CeRhSi_3$ agree with recent values from heat capacity.

caused by the possible existence of surface superconductivity sensed by resistivity measurements at low pressures, as has been suggested for $CeIrSi_3$ [31]. Very recent heat-capacity measurements in samples similar (grown with the same procedure and by the same group) to ours showed no sign of superconductivity below 1.8 GPa [32]. The low-pressure uncertainties in T_c do not affect the conclusions of the present study. For $CeIrSi_3$ we identify in Fig. 4(a) the critical pressures $p_c \approx 2.30$ GPa and $p_c^* \approx 2.60$ GPa, close to values reported earlier [11,12,33]. At the latter pressure AFM SDW vanishes (QCP), T_c is maximum, and several other properties indicate that superconductivity is optimal.

The AFM phase behaves quite remarkably in $CeRhSi_3$ [Fig. 4(b)]. The phase-boundary lines of the AFM and superconducting phases do not intercept but seem to merge at a pressure close to $p_c^* \approx 2.80$ GPa. Our data show no evidence of a $T = 0$ quantum phase transition in $CeRhSi_3$, at least in the pressure range studied. We could not detect any distinct sign of an AFM phase above 2.6 GPa, in agreement with previous results [29]. In an earlier report the AFM phase appears again under the application of a magnetic field of 4 T at 2.61 GPa [34], suggesting that the AFM order is hidden or suppressed by superconductivity at zero field.

B. Order parameter under pressure

Now, we discuss in detail the superconducting phase of both compounds starting with $CeIrSi_3$. The data in Figs. 2(a)–2(h) were limited to the superconducting region, converted to penetration depth, and then displayed in Fig. 5(a). Data were normalized to $\Delta\lambda_{max}$, defined as the total penetration-depth shift from T_c down to the lowest temperature. Low-temperature regions are expanded in Figs. 5(c) and 5(d). A conspicuous change of the penetration depth can be observed near p_c, both at the transition and at low temperatures. Remarkably, no qualitative change in $\lambda(T)$ is seen at the QCP. The most striking result, however, concerns the low-temperature behavior. Below p_c $\lambda(T)$ displays a linear temperature dependence [Fig. 5(c)], which indicates the presence of gapless quasiparticle excitations due to line nodes in the energy gap. The slope of the linear responses fades out as $p \to p_c$ and $\lambda(T)$ changes to an

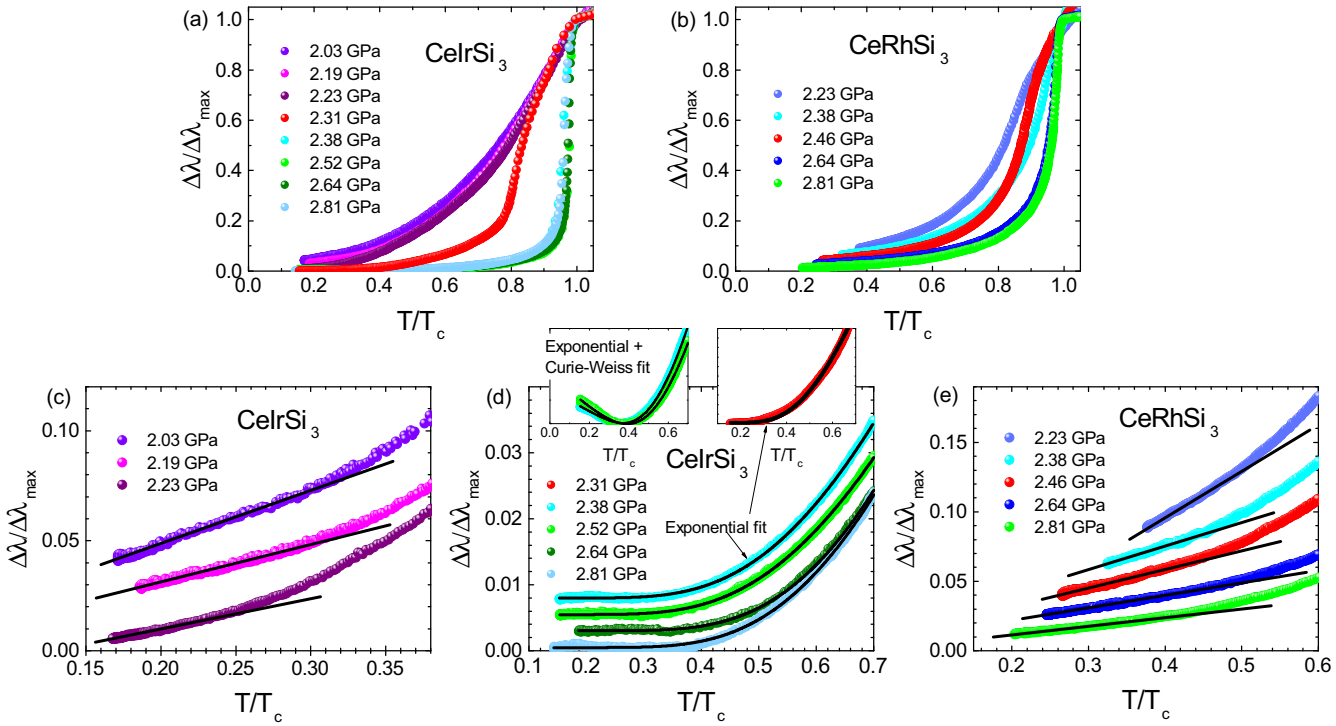

FIG. 5. Penetration depth of (a) $CeIrSi_3$ and (b) $CeRhSi_3$ under pressure. The transition widths decrease with pressure in both compounds. (c) Low-temperature data of $CeIrSi_3$ shows a linear behavior at $p < 2.30$ GPa. (d) $\lambda(T)$ of $CeIrSi_3$ changes smoothly to an exponential response at $p > p_c$. Left sided inset exhibits the low-temperature data for 2.52 and 2.64 GPa and the fits to BCS exponential function plus the Curie-Weiss law. Right sided inset displays the low-temperature data for 2.31 GPa. (e) Low-temperature $\lambda(T)$ of $CeRhSi_3$ behaves linearly at all applied pressures. No crossover to an exponential response is detected in $CeRhSi_3$. In (c), main panel of (d), and (e) data were shifted vertically for clarity.

exponential dependence [Fig. 5(d)], a characteristic behavior signaling the existence of an isotropic (nodeless) gap. The exponential dependence is seen at all applied pressures above p_c (at 2.38 and 2.52 GPa the Curie-Weiss component of the low-temperature signals was subtracted), even at the QCP where no further variation occurs. These results contradict the interpretation of ^{29}Si NMR data at 2.8 GPa in terms of line nodes [14], which could be due to the fact that NMR data were not taken at the low temperatures required to determine the gap structure.

On the other hand, near the AFM-SDW QCP T_c is maximal [Fig. 4(a)] and the transition width is minimal [Fig. 5(a)], which implies that superconductivity in $CeIrSi_3$ is optimal at this point. It is worth noting that transition widths have no relation with low-temperature behaviors (see the case of $CePt_3Si$ as an example [35]). When the gap is isotropic, the ratio Δ_0/k_BT_c is 2.14 at 2.31 GPa and 3.3 above this pressure. These values are higher than 1.76 expected from the BCS approach, suggesting contributions from strong-coupling corrections. All findings are in agreement with earlier results [12].

Following the same procedure as for $CeIrSi_3$, we consider $CeRhSi_3$. The penetration depth is presented in Fig. 5(b) and the low-temperature region is zoomed in Fig. 5(e). The superconducting transition sharpens as pressure increases up to $p_c^\star$ where T_c is maximal, very similar to that found in $CeIrSi_3$. However, $\lambda(T)$ always displays a linear dependence, which implies that the gap has line nodes at all studied pressures. Notably, the slope of the linear responses gets gradually smaller as pressure increases even slightly above $p_c^\star$.

We note here that the relative temperature ranges ($\Delta T/T_c$) at which $\lambda(T)$ of $CeIrSi_3$ and $CeRhSi_3$ behaves linearly are within those found in widely accepted experiments in UPt_3 [25], $CePt_3Si$ [17], $YBa_2Cu_3O_{7-x}$ [36], and $Bi_2Sr_2CaCu_2O_{8+x}$ [37].

Based on our findings we state that in $CeIrSi_3$ and $CeRhSi_3$ nodal superconductivity only appears in regions where $T_N \geqslant T_c$; i.e., where the magnetic energy scale dominates over the superconducting one. The transition from nodal to nodeless energy gap at p_c in $CeIrSi_3$ and the existence of line nodes in the absence of a $T = 0$ quantum phase transition in $CeRhSi_3$ provide experimental evidence that nodal superconductivity in these compounds seems to be related to the coexistence with a magnetic order. Another striking issue is that in both compounds superconductivity becomes strongest at $p_c^\star$ (also seen in heat-capacity and resistivity measurements [33]). The values of upper critical fields, zero-temperature energy gaps, and heat-capacity jumps, among others, suggest that at $p_c^\star$ (at the QCP in $CeIrSi_3$) superconductivity in these compounds is non-BCS and not driven by electron-phonon interactions. From our results the magnetic QCP may certainly play a role in the optimal superconductivity of $CeIrSi_3$.

C. Interpretation of the superconducting gap structure

The relationship between the gap structure (line nodes) and the dominant AFM order in $CeIrSi_3$ and $CeRhSi_3$ is intriguing. A possible scenario to understand this connection

could be based on the fact that the underlying symmetries of the electronic system are different with and without AFM order. The lower symmetry of the AFM state may lead to a reduced phase space for Cooper pairing favoring a nodal pairing state, whereas in the absence of AFM order Cooper pairs can take advantage of an enlarged set of possible pairing states enabling the condensate to avoid nodes. This viewpoint does not require a qualitative change of the pairing interaction which may originate from the same magnetic fluctuations associated with QCP. This recalls the discussion of the superconducting double transition observed in UPt_3 that may be connected to the slight lifting of the degeneracy in a multicomponent order parameter space due to AFM order, leading to a "high"-temperature phase with more nodes than the "low"-temperature phase [38]. This type of scenario results likely in a superconducting state which breaks time reversal symmetry for the nodeless phase, a feature which could be probed by zero-field μSR.

Another picture that may explain our findings can be based on the lack of inversion symmetry. Although antisymmetric spin-orbit coupling alone might not be responsible for unconventional superconductivity [39], it could combine with AFM order to cause the observed nodal gaps in these noncentrosymmetric superconductors, as suggested on theoretical grounds [40,41]. However, these studies ignore the complex nature of the heavy-fermion physics.

D. Possible implications for other heavy fermions

The results of the present study can be analyzed in the context of other heavy fermions in which superconductivity and magnetism coexist. Our results are consistent with those in $CePt_3Si$ [42] and $CeCu_2Si_2$ [43], which are two of the very few heavy fermions with consonant experimental outcomes. In noncentrosymmetric $CePt_3Si$, whose superconductivity coincides with antiferromagnetism from ambient pressure up to about 0.6 GPa, where the AFM phase vanishes at $T = 0$, the gap has line nodes at ambient pressure [17,44]. In stoichiometric $CeCu_2Si_2$ there is no coexistence of these phenomena under any hydrostatic pressure condition and the energy gap seems to be isotropic and robust against disorder [43,45]. Coexistence appears upon the substitution of small quantities of Si with Ge, corresponding to a lattice expansion and somehow to a negative chemical pressure [46,47]. Indeed, in $CeCu_2(Si_{0.9}Ge_{0.1})_2$ an AFM phase coincides with part of the low-pressure superconducting state from ambient pressure up to around 1 GPa. At slightly higher pressure another superconducting phase is present. No study has been performed on the order parameters of these two superconducting phases of $CeCu_2(Si_{0.9}Ge_{0.1})_2$. $CeCoIn_5$, on the other hand, appears to be at odd, since unconventional behaviors have been observed in the absence of coexistence of superconductivity and magnetism at ambient pressure [48,49]. Considering other systems different from heavy fermions such as iron pnictides and CrAs, with similar phase diagrams as the one of $CeIrSi_3$, the energy gap does not present any anomalous variation around an AFM QCP [6,8–10,50]. The difference may be that in iron pnictides magnetic order evolves from more itinerant d electrons.

IV. SUMMARY

We presented an experimental setup to study the superconducting gap structure under pressure. We studied the pressure evolution of the energy gaps of $CeIrSi_3$ and $CeRhSi_3$. In $CeIrSi_3$ we found a crossover from line node to isotropic gap at a pressure distinctively lower than that of the QCP. In $CeRhSi_3$ no $T = 0$ quantum phase transition was observed within our measurements and line nodes exist at all applied pressures. These results provide evidence that the nodal excitation gap of superconductivity of both compounds is connected with the AFM order rather than the QCP. In $CeIrSi_3$ superconductivity is optimal at the QCP.

ACKNOWLEDGMENTS

We appreciate assistance from F. Honda at the early stage of the pressure project. We value conversations with S. Saxena. We acknowledge support from the Venezuelan Institute for Scientific Research (IVIC) Grant No. 441. The work by N.K. was supported by JSPS KAKENHI Grant No. JP26400345.

[1] T. Moriya and K. Ueda, Adv. Phys. **49**, 555 (2000).
[2] K. Kuroki, J. Phys. Soc. Jpn. **75**, 051013 (2006).
[3] E. Abrahams and Q. Si, J. Phys.: Condens. Matter **23**, 223201 (2011).
[4] C. Pfleiderer, Rev. Mod. Phys. **81**, 1551 (2009).
[5] B. D. White, J. D. Thompson, and M. B. Maple, Physica C **514**, 246 (2015).
[6] K. Cho, M. Konczykowski, S. Teknowijoyo, M. A. Tanatar, Y. Liu, T. A. Lograsso, W. E. Straszheim, V. Mishra, S. Maiti, P. J. Hirschfeld *et al.*, Sci. Adv. **2**, e1600807 (2016).
[7] Z. Guguchia, A. Amato, J. Kang, H. Luetkens, P. K. Biswas, G. Prando, F. von Rohr, Z. Bukowski, A. Shengelaya, H. Keller *et al.*, Nat. Commun. **6**, 8863 (2015).
[8] K. Hashimoto, K. Cho, T. Shibauchi, S. Kasahara, Y. Mizukami, R. Katsumata, Y. Tsuruhara, T. Terashima, H. Ikeda, M. A. Tanatar *et al.*, Science **336**, 1554 (2012).
[9] R. T. Gordon, H. Kim, N. Salovich, R. W. Giannetta, R. M. Fernandes, V. G. Kogan, T. Prozorov, S. L. Budko, P. C. Canfield, M. A. Tanatar *et al.*, Phys. Rev. B **82**, 054507 (2010).
[10] F. Hardy, P. Burger, T. Wolf, R. A. Fisher, P. Schweiss, P. Adelmann, R. Heid, R. Fromknecht, R. Eder, D. Ernst *et al.*, Europhys. Lett. **91**, 47008 (2010).
[11] I. Sugitani, Y. Okuda, H. Shishido, T. Yamada, A. Thamizhavel, E. Yamamoto, T. D. Matsuda, Y. Haga, T. Takeuchi, R. Settai *et al.*, J. Phys. Soc. Jpn. **75**, 043703 (2006).
[12] N. Tateiwa, Y. Haga, T. D. Matsuda, S. Ikeda, E. Yamamoto, Y. Okuda, Y. Miyauchi, R. Settai, and Y. Ōnuki, J. Phys. Soc. Jpn. **76**, 083706 (2007).
[13] N. Kimura, K. Ito, K. Saitoh, Y. Umeda, H. Aoki, and T. Terashima, Phys. Rev. Lett. **95**, 247004 (2005).

[14] H. Mukuda, T. Fujii, T. Ohara, A. Harada, M. Yashima, Y. Kitaoka, Y. Okuda, R. Settai, and Y. Ōnuki, Phys. Rev. Lett. **100**, 107003 (2008).
[15] Y. Kitamura, T. Matsubara, Y. Machida, Y. Ōnuki, B. Salce, J. Flouquet, and K. Izawa, J. Phys. Conf. Ser. **592**, 012148 (2015).
[16] E. Bauer and M. Sigrist, *Non-Centrosymmetric Superconductors: Introduction and Overview*, Lecture Notes in Physics Vol. 847 (Springer-Verlag, Berlin, 2012).
[17] I. Bonalde, W. Brämer-Escamilla, and E. Bauer, Phys. Rev. Lett. **94**, 207002 (2005).
[18] S. Klotz, K. Takemura, T. Strässle, and T. Hansen, J. Phys.: Condens. Matter **24**, 325103 (2012).
[19] H. Yamaoka, Y. Zekko, I. Jarrige, J. F. Lin, N. Hiraoka, H. Ishii, K. D. Tsuei, and J. Mizuki, J. Appl. Phys. **112**, 124503 (2012).
[20] L. D. Jennings and C. A. Swenson, Phys. Rev. **112**, 31 (1958).
[21] N. B. Brandt and N. I. Ginzburg, Sov. Phys. JETP **23**, 838 (1966).
[22] A. B. Lidiard, Rep. Prog. Phys. **17**, 201 (1954).
[23] E. Fawcett, Rev. Mod. Phys. **60**, 209 (1988).
[24] T. Jacobs, B. A. Willemsen, S. Sridhar, R. Nagarajan, L. C. Gupta, Z. Hossain, C. Mazumdar, P. C. Canfield, and B. K. Cho, Phys. Rev. B **52**, R7022 (1995).
[25] S. Schottl, E. A. Schuberth, K. Flachbart, J. B. Kycia, J. I. Hong, D. N. Seidman, W. P. Halperin, J. Hufnagl, and E. Bucher, Phys. Rev. Lett. **82**, 2378 (1999).
[26] E. E. M. Chia, I. Bonalde, B. D. Yanoff, D. J. Van Harlingen, M. B. Salamon, S. I. Lee, and H. J. Kim, J. Magn. Magn. Mater. **226-230**, 301 (2001).
[27] E. E. M. Chia, W. Cheong, T. Park, M. B. Salamon, E. M. Choi, and S. I. Lee, Phys. Rev. B **72**, 214505 (2005).
[28] T. Park, F. Ronning, H. Q. Yuan, M. B. Salamon, R. Movshovich, J. L. Sarrao, and J. D. Thompson, Nature (London) **440**, 65 (2006).
[29] N. Kimura, K. Ito, H. Aoki, S. Uji, and T. Terashima, Phys. Rev. Lett. **98**, 197001 (2007).
[30] F. Tomioka, M. Hedo, I. Umehara, T. Ono, Y. Uwatoko, N. Kimura, and S. Takayanagi, J. Magn. Magn. Mater. **310**, 340 (2007).
[31] H. Iida, M. Sato, and N. Kimura, J. Phys. Soc. Jpn. **85**, 073708 (2016).
[32] I. Umehara (private communication).
[33] R. Settai, K. Katayama, D. Aoki, I. Sheikin, G. Knebel, J. Flouquet, and Y. Ōnuki, J. Phys. Soc. Jpn. **80**, 094703 (2011).
[34] H. Iida, T. Sugawara, H. Aoki, and N. Kimura, Phys. Status Solidi B **250**, 502 (2013).
[35] I. Bonalde, R. L. Ribeiro, K. J. Syu, H. H. Sung, and W. H. Lee, New J. Phys. **11**, 055054 (2009).
[36] W. N. Hardy, D. A. Bonn, D. C. Morgan, R. Liang, and K. Zhang, Phys. Rev. Lett. **70**, 3999 (1993).
[37] T. Jacobs, S. Sridhar, Q. Li, G. D. Gu, and N. Koshizuka, Phys. Rev. Lett. **75**, 4516 (1995).
[38] R. Joynt and L. Taillefer, Rev. Mod. Phys. **74**, 235 (2002).
[39] R. L. Ribeiro, I. Bonalde, Y. Haga, R. Settai, and Y. Ōnuki, J. Phys. Soc. Jpn. **78**, 115002 (2009).
[40] S. Fujimoto, J. Phys. Soc. Jpn. **75**, 083704 (2006).
[41] Y. Yanase and M. Sigrist, J. Phys. Soc. Jpn. **76**, 043712 (2007).
[42] N. Kimura and I. Bonalde, in *Non-Centrosymmetric Superconductors: Introduction and Overview*, edited by E. Bauer and M. Sigrist, Lecture Notes in Physics Vol. 847 [16], Chap. 2, pp. 35–79.
[43] T. Yamashita, T. Takenaka, Y. Tokiwa, J. A. Wilcox, Y. Mizukami, D. Terazawa, Y. Kasahara, S. Kittaka, T. Sakakibara, M. Konczykowski *et al.*, Sci. Adv. **3**, e1601667 (2017).
[44] K. Izawa, Y. Kasahara, Y. Matsuda, K. Behnia, T. Yasuda, R. Settai, and Y. Ōnuki, Phys. Rev. Lett. **94**, 197002 (2005).
[45] T. Takenaka, Y. Mizukami, J. A. Wilcox, M. Konczykowski, S. Seiro, C. Geibel, Y. Tokiwa, C. Putzke, Y. Matsuda, A. Carrington *et al.*, Phys. Rev. Lett. **119**, 077001 (2017).
[46] G. Sparn, O. Stockert, F. Grosche, H. Yuan, E. Faulhaber, C. Geibel, M. Deppe, H. Jeevan, M. Loewenhaupt, G. Zwicknagl *et al.*, J. Phys. Chem. Solids **67**, 529 (2006).
[47] F. Steglich, J. Phys. Conf. Ser. **400**, 022111 (2012).
[48] R. J. Ormeno, A. Sibley, C. E. Gough, S. Sebastian, and I. R. Fisher, Phys. Rev. Lett. **88**, 047005 (2002).
[49] E. E. M. Chia, D. J. Van Harlingen, M. B. Salamon, B. D. Yanoff, I. Bonalde, and J. L. Sarrao, Phys. Rev. B **67**, 014527 (2003).
[50] R. Khasanov, Z. Guguchia, I. Eremin, H. Luetkens, A. Amato, P. K. Biswas, C. Rüegg, M. A. Susner, A. S. Sefat, N. D. Zhigadlo *et al.*, Sci. Rep. **5**, 13788 (2015).